Model of the initiation of signal transduction by ligands in a cell culture: Simulation of molecules near a plane membrane comprising receptors

Ianik Plante and Francis A. Cucinotta

Phys. Rev. E **84**, 051920 — Published 28 November 2011

DOI: 10.1103/PhysRevE.84.051920

A. Title

Model of the initiation of signal transduction by ligands in a cell culture. Simulation of molecules near a plane membrane comprising receptors

B. Authors names

Ianik Plante[†‡] and Francis A. Cucinotta[†*]

C. Authors affiliations

[†]NASA Johnson Space Center
2101 NASA Parkway, Houston, TX 77058

[‡]Division of Space Life Sciences
Universities Space Research Association
3600 Bay Area Boulevard, Houston, TX 77058

Email: ianik.plante-1@nasa.gov
Francis.A.Cucinotta@nasa.gov

*Corresponding Author:

Francis A. Cucinotta
NASA Johnson Space Center
2101 NASA Parkway
Mail Code SK
Houston TX 77058
Office: 281 483-0968
Fax: 281 483-3058

D. Receipt date

July 8, 2011

E. Abstract

Cell communication is a key mechanism in tissue responses to radiation. Several molecules are implicated in radiation-induced signaling between cells, but their contributions to radiation risk is poorly understood. Meanwhile, Green functions for diffusion-influenced reactions have appeared in the literature, which are applied to describe the diffusion of molecules near a plane membrane comprising bound receptors with the possibility of reversible binding of a ligand and activation of signal transduction proteins by the ligand-receptor complex. We have developed Brownian Dynamics algorithms to simulate particles histories in this system, which can accurately reproduce the theoretical distribution of distances of a ligand from the membrane, the number of reversibly bound particles and the number of receptor complexes activating signaling proteins as a function of time, regardless of the number of timesteps used for the simulation. These simulations will be of great importance to model interactions at low doses where stochastic effects induced by a small number of molecules or interactions come into play.

F. Physics and Astronomy Classification Scheme (PACS) indexing codes

87.15.A- Theory, modeling, and computer simulation
87.15.ak Monte Carlo simulations
82.37.Np Single molecule reaction kinetics, dissociation, etc.
87.53.Ay Biophysical mechanisms of interaction

G. Main body of the paper

I. INTRODUCTION

An increasing number of experiments suggest that cells respond collectively rather than individually to radiation [1-2]. An example of this is the bystander effect, a phenomenon whereby cells that were not in direct contact with radiation are also affected [3]. A great number of so-called bystander or non-targeted effects of radiation have been observed experimentally, such as micronuclei formation [4], mutations [5], reduction in clonogenic survival [6], apoptosis [7], changes in transformation frequency [8], and tumor induction [9]. The underlying mechanisms that mediate these non-targeted effects are poorly understood, but they suggest that cell signaling plays a major role in the response of tissues to radiation. An example of the role of cell signaling is amplified autocrine signaling, which is one of the hallmarks of cancer [10]. Molecules such as transforming growth factor (TGFβ) [11], reactive oxygen species (ROS) [4], $NO^{\bullet}$ radical [12] and membrane-bound NADPH oxidases [13] have been implicated in radiation-induced signaling between cells.

To improve understanding of the mechanisms of cell signaling, computational models have been used to elucidate the interaction between the epidermal growth factor (EGF) and its receptor (EGFR) in a systems biology perspective [14-17]. In these models, a Brownian Dynamics (BD) algorithm which has been developed has been able to characterize the spatial range of secreted ligands and to discriminate the roles of autocrine and paracrine trajectories in cell culture. Over the years, increasingly sophisticated BD algorithms have appeared in the literature [18-22], which has been used to understand reversible chemical reactions kinetics. With appropriate modifications, these models and algorithms are the cornerstone of a computational model using reaction rate constants of receptors distributed on cell membranes that could allow a better understanding of cell communication in an irradiated system. Of importance is the ability to model interactions at low doses where stochastic effects induced by a small number of molecules or interactions come into play. Eventually, these simulations will allow us to calculate the range, lifetime and concentration of TGFβ following irradiation, as well as the number of cells affected by TGFβ and the positions where these molecules will bind to the cell surface receptors to initiate signal transduction.

In this paper, BD algorithms for the simulation of the motion of a particle near a plane membrane comprising receptors and initiation of signal transduction are discussed. In the first part of the paper, the Green functions (or propagators) describing a particle near a membrane with receptors under diffusion are reviewed, the most general case being a membrane comprising receptors with the possibility of dissociation of a bound ligand and activation of signal transduction by the ligand-receptor complex. In the second part, two very important aspects of the BD simulations not covered by previous papers, the discretization of time and the sampling of the Green functions, are examined. In regards to sampling of the Green functions, the algorithms described in this paper require a very low amount of memory or disk space and are computationally fast. Simulation results and how these simulations could be used to link radiation track structure models with existing DNA repair models to improve our understanding of the radiation risks are also discussed.

II. GREEN FUNCTIONS OF LIGAND INTERACTION WITH CELL SURFACE RECEPTORS

A. Cell culture model

Several investigators [14-17] model a cell culture as a «cylinder» of infinite radius[1] and of finite height[2] where ligand molecule can diffuse and bind to cells receptors. The surface at the top of the cell culture is totally reflective for the molecules. The bottom surface is covered by cells with receptors; the membrane is then partially absorbing for ligands. In this system, a particle in cell culture will follow stochastic trajectories according to the diffusion equation (DE), which can be written in 1D:

$$\frac{\partial p(x,t \mid x_0)}{\partial t} = D\frac{\partial^2}{\partial x^2} p(x,t \mid x_0) \tag{1}$$

Where $p(x,t|x_0)$ is the probability distribution function that a particle initially at $x_0>0$ is found at position x at time t and D is the diffusion coefficient of the ligand. For TGFβ, $D\sim 2.6\times10^{-7}$ cm^2/s (Table 1). The initial condition of the DE for a particle initially at $x=x_0$ can be written as $p(x,0|x_0)=\delta(x-x_0)$, where $\delta(x)$ is the Dirac's delta function. The solution $p(x,t|x_0)$ is the Green function [19].

Table 1

B. Reflective boundary at x=0

In our simulations, to simplify the analytical treatment, the height of the cell culture was assumed to be infinite. For a semi-infinite half-space (x>0) with a reflective boundary at x=0, the boundary condition is written as:

$$D\frac{\partial p(x,t \mid x_0)}{\partial x}\bigg|_{x=0} = 0 \tag{2}$$

The solution of the equation with the preceding initial and boundary conditions, which is referred to as $p_{ref}(x,t|x_0)$, is given by [18]:

$$p(x,t \mid x_0) = p_{ref}(x,t \mid x_0) = \frac{1}{\sqrt{4\pi Dt}}\left\{\exp\left[-\frac{(\mathbf{x}-\mathbf{x_0})^2}{4Dt}\right] + \exp\left[-\frac{(\mathbf{x}+\mathbf{x_0})^2}{4Dt}\right]\right\} \tag{3}$$

[1] The diffusion in the Y and Z directions can be considered as free diffusion in an infinite medium. This is a trivial problem and it will not be discussed further here. However, the diffusion in the Y and Z directions will be very important in the calculations of autocrine and paracrine range of ligand interaction.

[2] In practice, the height of a cell culture (~2 mm) is much greater than the typical distance travelled by a particle in a time-step; therefore, the height of the cell culture is also considered infinite in this work.

The survival probability of a particle $Q(t|x_0)$ is given by the integration of $p_{ref}(x,t|x_0)$ over the half-space $[0,\infty)$. It is 1 for every $t>0$ in this case.

$$Q(t \mid x_0) = \int_0^\infty p(x,t \mid x_0)dx = 1 \tag{4}$$

C. Partially absorptive boundary at x=0

In the cell culture model, the boundary condition on the surface of the cells is given by

$$D\frac{\partial p(x,t \mid x_0)}{\partial x}\bigg|_{x=0} = k_a p(0,t \mid x_0) \tag{5}$$

where k_a is the rate constant in m/s. The membrane absorption constant k_a can be linked to the ligand-receptor binding rate constant k_{on} (in $M^{-1}s^{-1}$) by $k_a=k_{on}R_{total}/(\pi R_{cell}^2 N_A)$ [14], where N_A is Avogadro's number, R_{total} is the number of receptors at the cell surface and R_{cell} is the cell radius. Typically, for the TGFβ system, $k_{on}=(2.3\pm0.2)\text{x}10^7$ $M^{-1}s^{-1}$ and R_{total}~1000 receptors/cell [24]. This yields $k_a=1.95\text{x}10^{-6}$ cm/s (Table 2).

Table 2

This boundary condition applies only to the surface covered by cells, whereas the reflecting boundary condition applies elsewhere. It is very difficult to obtain an analytical solution in such a case. To simplify the analytical treatment, the surface is homogenized, i.e., the receptors are assumed to be uniformly distributed on the surface rather than on the cells only [16,25]. The rate constant k_a is replaced in equation (5) by an effective rate constant κ_{eff} (m/s), which can be calculated from the following equation [14]:

$$\kappa_{eff} = \frac{k_a \sigma}{1 + \pi k_a R_{cell}/4D} \tag{6}$$

where σ is the fraction of the surface which is covered by cells. For convenience, the notation k_a will be kept throughout this text. The Green function for a particle initially at a distance x_0 from the membrane is [18]:

$$p(x,t \mid x_0) = p_{ref}(x,t \mid x_0) - \alpha W\left(\frac{x+x_0}{\sqrt{4Dt}}, \alpha\sqrt{Dt}\right) \tag{7}$$

where $\alpha=k_a/D$. and the functions $W(a,b)$[3] and $\Omega(b)$ are defined as follow:

$$\Omega(x) = e^{x^2}\,\mathrm{Erfc}(x) \tag{8a}$$

$$W(a,b) \equiv \exp(2ab+b^2)\mathrm{Erfc}(a+b) = e^{-a^2}\Omega(a+b) \tag{8b}$$

[3] These functions may be difficult to evaluate numerically. The arguments of these functions may also be complex numbers. For complex arguments, the Faddeeva function is used [26].

Erfc(x) is the complementary error function:

$$\mathrm{Erfc}(x) = \frac{2}{\sqrt{\pi}} \int_x^\infty e^{-\xi^2} d\xi \tag{9}$$

The probability of a particle initially at x_0 to remain free at time t is obtained by integrating (7) over the half-space $[0,\infty)$:

$$Q(t \mid x_0) = \int_0^\infty p(x,t \mid x_0) dx = 1 - W\left(\frac{x_0}{\sqrt{4Dt}}, 0\right) + W\left(\frac{x_0}{\sqrt{4Dt}}, \alpha\sqrt{Dt}\right) \tag{10}$$

The probability $Q(t|x_0)$ is less than 1, indicating that a particle may bind to a receptor on the surface. If $t\to\infty$, $Q\to 0$, meaning that all particles will eventually bound to the membrane. The probability of a particle to occupy a bound state, noted (*), at time t is $p(*,t|x_0)=1-Q(t|x_0)$.

D. Reversible binding with membrane at x=0

The boundary condition (5) does not include the possible dissociation of a ligand from a receptor bound state (at x=0). This effect has been included in previous chemistry-related calculations [19-20], but not in cell culture models. A particle can either be found in the semi-infinite half-space x>0 or occupy a bound state (at x=0), which will be noted (*). The central assumption is that the rate of desorption is proportional to the total absorbed population of particles $p(*,t|x_0)=1-Q(t|x_0)$. Hence the boundary condition at x=0 can be written as

$$D \left.\frac{\partial p(x,t \mid x_0)}{\partial x}\right|_{x=0} = k_a p(0,t \mid x_0) - k_d p(*,t \mid x_0) \tag{11}$$

where k_d is the dissociation constant. The units of k_d are s^{-1}, since dissociation is a first-order process. For the TGFβ system, $k_d \sim (1.5\pm 0.2)\times 10^{-4}\ s^{-1}$ [24]. The time evolution of the probability of a particle to be found in a bound state is given by [22]:

$$\frac{dp(*,t \mid x_0)}{dt} = k_a p(0,t \mid x_0) - k_d p(*,t \mid x_0) \tag{12}$$

This system can be solved analytically by Laplace transforms [19]. In this case, $p(x,t|x_0)$ takes the form:

$$p(x,t \mid x_0) = p_{ref}(x,t \mid x_0) - \frac{\alpha(\alpha+\beta)}{\alpha-\beta} W\left(\frac{x+x_0}{\sqrt{4Dt}}, \alpha\sqrt{Dt}\right) + \frac{\beta(\alpha+\beta)}{\alpha-\beta} W\left(\frac{x+x_0}{\sqrt{4Dt}}, \beta\sqrt{Dt}\right) \tag{13}$$

Where $\Delta^2=k_a^2-4Dk_d$, $\alpha=(k_a+\Delta)/2D$ and $\beta=(k_a-\Delta)/2D$. The probability of a free particle to remain in a free state is given by integration of equation (13):

$$Q(t \mid x_0) = 1+\left(\frac{\alpha+\beta}{\alpha-\beta}\right)\left[W\left(\frac{x_0}{\sqrt{4Dt}}, \alpha\sqrt{Dt}\right) - W\left(\frac{x_0}{\sqrt{4Dt}}, \beta\sqrt{Dt}\right)\right] \tag{14}$$

The probability of a particle initially at $x_0>0$ (free) to be found in a bound state at time t is thus $1-Q(t|x_0)$. That is:

$$p(*,t \mid x_0) = -\left(\frac{\alpha+\beta}{\alpha-\beta}\right)\left[W\left(\frac{x_0}{\sqrt{4Dt}}, \alpha\sqrt{Dt}\right) - W\left(\frac{x_0}{\sqrt{4Dt}}, \beta\sqrt{Dt}\right)\right] \tag{15}$$

A ligand-receptor complex may dissociate. The probability distribution of a particle initially in a bound state to be found at position $x>0$ at time t is found by using the material balance condition $k_a p(x,t|*)=k_d p(*,t|x)$ (see ref. [22]). Using $\alpha\beta=k_d/D$ and $\alpha-\beta=\Delta/D$, one finds [21]:

$$p(x, t \mid *) = \frac{\alpha\beta}{\alpha-\beta}\left[W\left(\frac{x}{\sqrt{4Dt}}, \beta\sqrt{Dt}\right) - W\left(\frac{x}{\sqrt{4Dt}}, \alpha\sqrt{Dt}\right)\right] \tag{16}$$

The probability of dissociation from the bound state is given by integration of equation (16):

$$Q(t \mid *) = 1+\frac{1}{\alpha-\beta}\left[\beta\Omega\left(\alpha\sqrt{Dt}\right) - \alpha\Omega\left(\beta\sqrt{Dt}\right)\right] \tag{17}$$

The probability of a bound particle to remain bound at time t is $p(*,t|*)=1-Q(t|*)$:

$$p(*, t \mid *) = \frac{1}{\alpha-\beta}\left[\alpha\Omega\left(\beta\sqrt{Dt}\right) - \beta\Omega\left(\alpha\sqrt{Dt}\right)\right] \tag{18}$$

E. Reversible recombination with membrane and initiation of signal transduction

A ligand receptor complex will either dissociate or initiate signal transduction by activating proteins such as the Smad proteins in the case of TGFβ. As a first approximation, this is equivalent to the problem

$$A + B \underset{k_d}{\overset{k_a}{\rightleftarrows}} (AB)^* \xrightarrow{k_e} AB \tag{19}$$

In our model, the rate constant k_e corresponds to the pathway that a receptor-ligand complex will use to initiate action. For the TGFβ and its receptor, $k_e \sim 0.05\ s^{-1}$. The boundary condition is also given by equation (11). However, the time evolution of the reversibly bound state is given by:

$$\frac{dp(*,t \mid x_0)}{dt} = k_a p(0,t \mid x_0) - (k_d + k_e) p(*,t \mid x_0) \tag{20}$$

Similarly, the time evolution for the irreversibly bound state at time t, is given by:

$$\frac{dp(**,t \mid x_0)}{dt} = k_e p(*,t \mid x_0) \tag{21}$$

This state will be noted (∗∗) and corresponds to activation of signal transduction in our model.

This problem can be solved analytically using Laplace Transforms [22]. The solutions are expressed using three coefficients α, β and γ. They are the roots of a cubic polynomial[4] which depends on the rate constants k_a, k_d and k_e as follow:

$$\alpha + \beta + \gamma = k_a / D \tag{22a}$$

$$\alpha\beta + \beta\gamma + \gamma\alpha = (k_e + k_d)/D \tag{22b}$$

$$\alpha\beta\gamma = k_e k_a / D^2 \tag{22c}$$

The Green function for a free particle for this system is given by [22]:

$$\begin{aligned} p(x,t \mid x_0) &= p_{ref}(x,t \mid x_0) + \frac{\alpha(\gamma+\alpha)(\alpha+\beta)}{(\gamma-\alpha)(\alpha-\beta)} W\left(\frac{x+x_0}{\sqrt{4Dt}}, \alpha\sqrt{Dt}\right) \\ &+ \frac{\beta(\alpha+\beta)(\beta+\gamma)}{(\alpha-\beta)(\beta-\gamma)} W\left(\frac{x+x_0}{\sqrt{4Dt}}, \beta\sqrt{Dt}\right) + \frac{\gamma(\beta+\gamma)(\gamma+\alpha)}{(\beta-\gamma)(\gamma-\alpha)} W\left(\frac{x+x_0}{\sqrt{4Dt}}, \gamma\sqrt{Dt}\right) \end{aligned} \tag{23}$$

As usual, the probability of a particle initially at $x_0>0$ to remain in a free state $Q(t|x_0)$ is obtained by integrating equation (23):

$$\begin{aligned} Q(t \mid x_0) &= 1 - \frac{(\gamma+\alpha)(\alpha+\beta)}{(\gamma-\alpha)(\alpha-\beta)} W\left(\frac{x_0}{\sqrt{4Dt}}, \alpha\sqrt{Dt}\right) - \frac{(\alpha+\beta)(\beta+\gamma)}{(\alpha-\beta)(\beta-\gamma)} W\left(\frac{x_0}{\sqrt{4Dt}}, \beta\sqrt{Dt}\right) \\ &- \frac{(\beta+\gamma)(\gamma+\alpha)}{(\beta-\gamma)(\gamma-\alpha)} W\left(\frac{x_0}{\sqrt{4Dt}}, \gamma\sqrt{Dt}\right) - W\left(\frac{x_0}{\sqrt{4Dt}}, 0\right) \end{aligned} \tag{24}$$

The probability of a particle initially at $x_0>0$ to reversibly bound at time t (*) is [22]:

$$\begin{aligned} p(*,t \mid x_0) &= \frac{\alpha(\alpha+\beta+\gamma)}{(\gamma-\alpha)(\alpha-\beta)} W\left(\frac{x_0}{\sqrt{4Dt}}, \alpha\sqrt{Dt}\right) + \frac{\beta(\alpha+\beta+\gamma)}{(\alpha-\beta)(\beta-\gamma)} W\left(\frac{x_0}{\sqrt{4Dt}}, \beta\sqrt{Dt}\right) \\ &+ \frac{\gamma(\alpha+\beta+\gamma)}{(\beta-\gamma)(\gamma-\alpha)} W\left(\frac{x_0}{\sqrt{4Dt}}, \gamma\sqrt{Dt}\right) \end{aligned} \tag{25}$$

[4] At least one of the roots of a 3rd order polynomial is real, the two other roots being either both real or complex conjugates.

A particle initially at $x_0>0$ can also be found in an irreversibly bound state at time t. The probability to be found in this state is given by $p(**,t|x_0)=1-p(*,t|x_0)-Q(t|x_0)$. This calculation gives:

$$p(**,t\mid x_0)=\frac{\beta\gamma}{(\gamma-\alpha)(\alpha-\beta)}W\left(\frac{x_0}{\sqrt{4Dt}},\alpha\sqrt{Dt}\right)+\frac{\alpha\gamma}{(\alpha-\beta)(\beta-\gamma)}W\left(\frac{x_0}{\sqrt{4Dt}},\beta\sqrt{Dt}\right)$$
$$+\frac{\alpha\beta}{(\beta-\gamma)(\gamma-\alpha)}W\left(\frac{x_0}{\sqrt{4Dt}},\gamma\sqrt{Dt}\right)+W\left(\frac{x_0}{\sqrt{4Dt}},0\right) \quad (26)$$

To obtain the Green function of a particle in a reversibly bound state, the material balance condition $k_a p(x,t|*)=k_d\, p(*,t|x)$ [21-22] is used. This yields

$$\frac{D}{k_d}p(x,t\mid *)=\frac{\alpha}{(\gamma-\alpha)(\alpha-\beta)}W\left(\frac{x}{\sqrt{4Dt}},\alpha\sqrt{Dt}\right)+\frac{\beta}{(\alpha-\beta)(\beta-\gamma)}W\left(\frac{x}{\sqrt{4Dt}},\beta\sqrt{Dt}\right)$$
$$+\frac{\gamma}{(\beta-\gamma)(\gamma-\alpha)}W\left(\frac{x}{\sqrt{4Dt}},\gamma\sqrt{Dt}\right) \quad (27)$$

The probability of dissociation for a particle that was initially in a reversibly bound state $Q(t|*)$ is found by integrating equation (27):

$$\frac{D}{k_d}Q(t\mid *)=-\frac{1}{(\gamma-\alpha)(\alpha-\beta)}\Omega\left(\alpha\sqrt{Dt}\right)-\frac{1}{(\alpha-\beta)(\beta-\gamma)}\Omega\left(\beta\sqrt{Dt}\right)-\frac{1}{(\beta-\gamma)(\gamma-\alpha)}\Omega\left(\gamma\sqrt{Dt}\right) \quad (28)$$

The probability of a particle initially in a reversibly bound state to remain in this state during t is given by [22]:

$$p(*,t\mid *)=\frac{\alpha(\beta+\gamma)}{(\gamma-\alpha)(\alpha-\beta)}\Omega\left(\alpha\sqrt{Dt}\right)+\frac{\beta(\gamma+\alpha)}{(\alpha-\beta)(\beta-\gamma)}\Omega\left(\beta\sqrt{Dt}\right)+\frac{\gamma(\alpha+\beta)}{(\beta-\gamma)(\gamma-\alpha)}\Omega\left(\gamma\sqrt{Dt}\right) \quad (29)$$

Finally, the probability of an initially bound particle to activate signal transduction is $p(**,t|*)=1-Q(t|*)-p(*,t|*)$. Using $k_d/D=(\alpha+\beta)(\beta+\gamma)(\gamma+\alpha)/(\alpha+\beta+\gamma)$, $p(**,t|*)$ can be written:

$$p(**,t\mid *)=1+\frac{1}{\alpha+\beta+\gamma}\left[\frac{\beta\gamma(\beta+\gamma)}{(\gamma-\alpha)(\alpha-\beta)}\Omega\left(\alpha\sqrt{Dt}\right)+\frac{\alpha\gamma(\alpha+\gamma)}{(\alpha-\beta)(\beta-\gamma)}\Omega\left(\beta\sqrt{Dt}\right)+\frac{\alpha\beta(\alpha+\beta)}{(\beta-\gamma)(\gamma-\alpha)}\Omega\left(\gamma\sqrt{Dt}\right)\right] \quad (30)$$

In sections (II-D) and (II-E), according to the values of α, β and γ, the Green functions may have singularities (0/0) called transitions, which may lead to several computational issues. They are discussed in Appendix A.

III. DISCRETIZATION OF TIME

A simulation is usually divided in a finite number of timesteps Δt. Let $p(x,t|x_0)$ be the probability distribution for a particle to be at position x after the time t. If the simulation can be done in two timesteps such as timesteps $t=\Delta t_1+\Delta t_2$, we should have

$$p(x,t \mid x_0) = \int_{\Omega} p(x,\Delta t_2 \mid x_1) p(x_1,\Delta t_1 \mid x_0) dx_1 \tag{31}$$

Where Ω is the domain of x, i.e. the interval $[0,\infty)$. This is the Chapman-Kolmogorov equation. That is, the probability to find the particle at x after one timestep t is the same as the probability to find the particle at x after two timesteps Δt_1 and Δt_2, going through an intermediate position x_1. Time discretization is an important aspect to consider in simulation. For example, in radiation chemistry simulations, the results should be independent of the number and magnitude of timesteps, if the timesteps are reasonably small [27].

In the following sections, we discuss how the Chapman-Kolmogorov equation should be modified for the different cases considered in this paper. In most cases, we were not able to perform these integrals by using the analytical forms of the Green functions. However, because the processes considered in this paper are Markov processes, it immediately follows that Chapman-Kolmogorov type equations do hold. Equation (31) can be verified by noting that the right-hand side satisfies the diffusion equation and the boundary condition at x=0 and x=infinity, and reduces to $p(x,\Delta t_1|x_0)$ for $\Delta t_2 \rightarrow 0$. Since the proof of these equations can be long, they are included in the supplementary documents accompanying this article [28-29].

A. Reflective boundary at x=0

For $p_{ref}(x,t|x_0)$, the right side of the equation (31) is the sum of four Gaussian integrals, which can be evaluated analytically [28]. The calculation is in agreement with equation (31) and confirms the assumption of time discretization for the reflective boundary at x=0.

B. Partially absorptive boundary at x=0

In this case, a free particle initially at x_0 can 1) go to an intermediate position x_1 during Δt_1 and then go to its final x position at Δt_2, 2) bind to the membrane during Δt_1 or 3) go to an intermediate position x_1 during Δt_1 and bind to the membrane during Δt_2. The first possibility can be written:

$$p(x,t \mid x_0) = \int_{\Omega} p(x,\Delta t_2 \mid x_1) p(x_1,\Delta t_1 \mid x_0) dx_1 \tag{32}$$

The probability to find a particle bound at $t=\Delta t_1+\Delta t_2$ will be given by the sum of 2) and 3):

$$p(*,t \mid x_0) = p(*,\Delta t_1 \mid x_0) + \int_\Omega p(*,\Delta t_2 \mid x_1)p(x_1,\Delta t_1 \mid x_0)dx_1 \quad (33)$$

As shown in the supporting document 2, equation (32) is also a solution of the DE and satisfies the boundary condition (5). Moreover, equation (33) can be deduced from equation (32). This integral has not been found in existing tables of integrals [30] and the software Mathematica was not able to solve it analytically. However, numerical integration was attempted for different values of x_0, x, D, Δt_1 and Δt_2 and k_a. For all values that were used, equations (32-33) were found to be true [28].

C. Reversible binding with membrane at x=0

In this case, a particle initially at the position $x_0>0$ can 1) go to an intermediate position x_1 during Δt_1 and then go to its final x position at Δt_2, 2) bind to the membrane during Δt_1 and stay bound during Δt_2, 3) bind to the membrane during Δt_1 and dissociate during Δt_2, 4) go to an intermediate position x_1 during Δt_1 and bind to the membrane during Δt_2. The probability distribution of a free particle at $t=\Delta t_1+\Delta t_2$ is given by:

$$p(x,t \mid x_0) = \int_\Omega p(x,\Delta t_2 \mid x_1)p(x_1,\Delta t_1 \mid x_0)dx_1 + p(x,\Delta t_2 \mid *)p(*,\Delta t_1 \mid x_0) \quad (34)$$

In this case, a term is added to the Chapman-Kolmogorov equation to take into account the contribution from the dissociation of bound particles after a timestep. Similarly, the probability of binding of a particle initially at x_0 at $t=\Delta t_1+\Delta t_2$ is given by:

$$p(*,t \mid x_0) = p(*,\Delta t_2 \mid *)p(*,\Delta t_1 \mid x_0) + \int_\Omega p(*,\Delta t_2 \mid x_1)p(x_1,\Delta t_1 \mid x_0)dx_1 \quad (35)$$

in the same way, a initially bound particle can 1) dissociate during Δt_1 and move to its final x position at Δt_2, 2) stay bound during Δt_1 and dissociate during Δt_2, 3) dissociate during Δt_1 and re-bind during Δt_2 or 4) stay bound during Δt_1 and Δt_2. This yields the time discretization equations for initially bound particles:

$$p(x,t \mid *) = \int_\Omega p(x,\Delta t_2 \mid x_1)p(x_1,\Delta t_1 \mid *)dx_1 + p(x,\Delta t_2 \mid *)p(*,\Delta t_1 \mid *) \quad (36)$$

$$p(*,t \mid *) = p(*,\Delta t_2 \mid *)p(*,\Delta t_1 \mid *) + \int_\Omega p(*,\Delta t_2 \mid x_1)p(x_1,\Delta t_1 \mid *)dx_1 \quad (37)$$

In the supplementary material [29], we verify that equation (34) satisfies the DE and the boundary condition (11), and that equations (35-37) can be deduced from equation (34). Furthermore, these equations were also verified numerically for all values of x_0, x, D, Δt_1, Δt_2, k_a and k_d that were tried [28].

D. Reversible recombination with membrane and initiation of signal transduction

In this case, the particle initially at the position x_0 can follow one of the following possibilities:
1) go to position x_1 during Δt_1 and then go to its final x position during Δt_2,
2) go to position x_1 during Δt_1 and reversibly to the membrane during Δt_2,
3) go to position x_1 during Δt_1 and activate signal transduction during Δt_2,
4) bind reversibly to the membrane during Δt_1 and stay in this state during Δt_2,
5) bind reversibly to the membrane during Δt_1 and dissociate during Δt_2,
6) bind reversibly to the membrane during Δt_1 and activate signal transduction during Δt_2, or
7) activate signal transduction during Δt_1.

From this system the following time discretization equations are obtained:

$$p(x,t \mid x_0) = \int_\Omega p(x,\Delta t_2 \mid x_1)p(x_1,\Delta t_1 \mid x_0)dx_1 + p(x,\Delta t_2 \mid *)p(*,\Delta t_1 \mid x_0) \quad (38)$$

$$p(*,t \mid x_0) = p(*,\Delta t_2 \mid *)p(*,\Delta t_1 \mid x_0) + \int_\Omega p(*,\Delta t_2 \mid x_1)p(x_1,\Delta t_1 \mid x_0)dx_1 \quad (39)$$

$$p(**,t \mid x_0) = p(**,\Delta t_1 \mid x_0) + p(**,\Delta t_2 \mid *)p(*,\Delta t_1 \mid x_0) + \int_\Omega p(**,\Delta t_2 \mid x_1)p(x_1,\Delta t_1 \mid x_0)dx_1 \quad (40)$$

Once again, a term is added to the Chapman-Kolmogorov equation to take into account the possibility of dissociation. Each term in the equations (38-40) corresponds to the possibilities 1)-7). Similarly, a particle initially in a reversibly bound state can:

1) dissociate to position x_1 during Δt_1 and go to its final position x during Δt_2,
2) dissociate to position x_1 during Δt_1 and re-bind reversibly during Δt_2,
3) dissociate to position x_1 during Δt_1 and initiate signal transduction during Δt_2,
4) stay bound reversibly during Δt_1 and dissociate to position x during Δt_2,
5) stay bound reversibly during Δt_1 and Δt_2,
6) stay bound reversibly during Δt_1 and initiate signal transduction during Δt_2, or
7) initiate signal transduction during Δt_1.

This yields the time discretization equations for the bound particle:

$$p(x,t \mid *) = \int_\Omega p(x,\Delta t_2 \mid x_1)p(x_1,\Delta t_1 \mid *)dx_1 + p(x,\Delta t_2 \mid *)p(*,\Delta t_1 \mid *) \quad (41)$$

$$p(*,t \mid *) = p(*,\Delta t_2 \mid *)p(*,\Delta t_1 \mid *) + \int_\Omega p(*,\Delta t_2 \mid x_1)p(x_1,\Delta t_1 \mid *)dx_1 \quad (42)$$

$$p(**,t \mid *) = p(**,\Delta t_1 \mid *) + p(**,\Delta t_2 \mid *)p(*,\Delta t_1 \mid *) + \int_\Omega p(**,\Delta t_2 \mid x_1)p(x_1,\Delta t_1 \mid *)dx_1 \quad (43)$$

Once again, we were not able to perform these integrals analytically by using the Green functions. However, in the supplementary material [29], we show that equation (38) is solution of the DE and of the boundary conditions and that equations (39-43) can be deduced from equation (38). Furthemore, numerical integration was also done for fixed

values of x_0, x, D, Δt_1, Δt_2, k_a, k_d and k_e. For all values that were used, equations (38-43) were found to be true [28].

IV. MONTE-CARLO SAMPLING OF THE GREEN FUNCTION (BROWNIAN DYNAMICS ALGORITHM)

In this section, the sampling algorithms of the propagators are discussed. They are used to calculate the state and position of a particle after a timestep Δt. In the limit of a infinite number of particles, many different algorithms are consistent. For a finite number of particles, the algorithms are not all equivalent. Those which are shown here are simple, fast and do not require much memory. For instance, the simulation of one time-step for 10^6 particles histories requires ~30 s and a few kilobytes of memory. Similar recent calculations [23] uses look-up tables comprising 20000 bins to sample the Green functions, which certainly require a large pre-calculation time and storage space.

A. Reflective boundary at x=0

A method for sampling x distributed as $p_{ref}(x,\Delta t|x_0)$ has been published in the 1980's [18], but it will be recalled here because it is needed to sample the other Green functions. Because $p_{ref}(x,\Delta t|x_0)$ is the sum of two Gaussian functions and is normalized to 1, a random X value distributed as $p_{ref}(x,\Delta t|x_0)$ can be generated by using a composition method [31]. The algorithm is the following:

BEGIN

Calculate $N_0 = \frac{1}{2}\mathrm{erfc}\left[-x_0/\sqrt{4D\Delta t}\right]$

Generate uniform [0,1] random variates U,V

IF ($U<N_0$)

$$X = x_0 + \sqrt{4D\Delta t}\,\mathrm{Erfc}^{-1}\left[V\mathrm{Erfc}\left(\frac{-x_0}{\sqrt{4D\Delta t}}\right)\right]$$

ELSE

$$X = -x_0 + \sqrt{4D\Delta t}\,\mathrm{Erfc}^{-1}\left[V\mathrm{Erfc}\left(\frac{x_0}{\sqrt{4D\Delta t}}\right)\right]$$

ENDIF

RETURN X ■

This algorithm gives a simple way to sample position x distributed as $p_{ref}(x,t|x_0)$. Tables 1 and 2 list the parameter values used in our simulations. On Figure 1, the probability distribution $p_{ref}(x,t|x_0)$ of a particle initially at x_0=2.5 is shown for t = 1, 2, 4, 8 and 16 (for convenience, dimensionless units have been used). We have simulated 10^6 histories of particles initially at x_0=2.5 by using the above algorithm to sample the position. The positions after 1, 2, 4, 8 and 16 time-steps of 1 unit are stored in normalized histograms.

Results are shown on Figure 1 for comparison. Similar results (not shown) are obtained regardless of the number of time-steps used; they match exactly the predicted analytical results and corroborate our assumption of time discretization.

Figure 1

B. Partially absorptive boundary at x=0

In this case, the propagator $p(x,\Delta t|x_0)$ is **not** normalized to 1. The first step is to verify if the particle is free after Δt. A uniform random number U is drawn and compared to $Q(\Delta t|x_0)$. If $U>Q(\Delta t|x_0)$, the particle is bound irreversibly to the membrane and no further treatment is necessary. If $U<Q(\Delta t|x_0)$, the particle is free and its new position is calculated as follows. By selecting only surviving particles, the propagator becomes normalized. By setting

$$p_2(x,\Delta t \mid x_0) = -\alpha W\left(\frac{x+x_0}{\sqrt{4D\Delta t}}, \alpha\sqrt{D\Delta t}\right) \tag{44}$$

we have $p_2(x,\Delta t|x_0)<0$ because $\alpha>0$. Thus, $p(x,\Delta t|x_0)$ respects the condition to use the negative mixture algorithm of Bignami and de Mattels [32], described in Appendix B. In this particular case, a random variate X with density $\sum_i p_{i+} f_i(x) / \sum_i p_{i+}$ is obtained by sampling $p_{ref}(x,\Delta t|x_0)$ as described in section 4.1. At each time-step, the probability of survival of a particle must be assessed before sampling the position X. The simulation results are shown on Figure 2.

Figure 2

In this figure, the probability distribution of a particle initially at $x_0=2.5$ with diffusion coefficient D=1 is shown after 1, 2, 4, 8 and 16 units. The simulation of 10^6 particles initially at $x_0=2.5$ using the algorithm is also shown for comparison. The results are the same regardless of the time-step used; they match very well the analytical results. On the right figure, the survival and binding probability of a particle initially at $x_0=2.5$ are shown for $k_a=0.1$, 1.0 and 10.0. It is well know that a particle, in 1D, will *always* reach the position x=0 if given sufficient time. Thus, the particle will *always* bind irreversibly after some time. This explains why the survival probability of a particles asymptotically decays to 0.

C. Partially absorptive boundary with dissociation at x=0

In this case, a particle can be free or reversibly bound; since the propagators are different in both situations, they should be treated differently. The first step is to determine whether a particle will be in a free or bound state after a time-step Δt. This is done by generating a random number and comparing it to the probability of survival $Q(\Delta t|x_0)$ for a free particle or to the probability of dissociation $Q(\Delta t|*)$ for a bound particle. If a particle is in a bound state after Δt, the treatment is over for this timestep. If a particle initially in

a free state remains in a free state, a position distributed as $p(x,\Delta t|x_0)$ should be sampled. By setting

$$p_2(x,\Delta t \mid x_0) = -\frac{\alpha(\alpha+\beta)}{\alpha-\beta} W\left(\frac{x+x_0}{\sqrt{4D\Delta t}}, \alpha\sqrt{D\Delta t}\right) + \frac{\beta(\alpha+\beta)}{\alpha-\beta} W\left(\frac{x+x_0}{\sqrt{4D\Delta t}}, \beta\sqrt{D\Delta t}\right) \quad (45)$$

we note that $p_2(x,\Delta t|x_0)\leq 0$. Therefore the algorithm of Bignami and de Mattels (Appendix B) [32] can be used. If a particle initially in a bound state dissociates, its position after Δt is found by sampling $p(x,\Delta t|*)$, which can be written:

$$p(x,\Delta t \mid *) = \frac{\alpha\beta}{\alpha-\beta}\exp\left(-\frac{x^2}{4D\Delta t}\right)\left[\Omega\left(\frac{x}{\sqrt{4D\Delta t}}+\beta\sqrt{D\Delta t}\right)-\Omega\left(\frac{x}{\sqrt{4D\Delta t}}+\alpha\sqrt{D\Delta t}\right)\right] \quad (46)$$

This form is very convenient because its last term is the product of a Gaussian-type function with the function $\Omega(x)$, which is ≤ 1 for $x\geq 0$. Since $\alpha\geq\beta$, the term inside brackets is ≤ 1. Thus, $p(x,\Delta t|*)$ is the product of a Gaussian function and a function ≤ 1; it can be sampled by a rejection method [31]. On Figure 3 (left), the probability distribution of a particle initially at $x_0=2.5$ for $k_a=5$ and $k_d=1$ is shown for t=1,2,4,8 and 16 units. The dots are simulation results, which can also be obtained by using various combination of time-steps. On the right figure, the probability of a given particle initially at $x_0=2.5$ to be free or reversibly bound is shown for $k_a=5$ and $k_d=0.1$, 1.0 and 10.0. In all cases, as discussed by [19], the particle will eventually be free as $t\rightarrow\infty$.

Figure 3

D. Reversible recombination with membrane and initiation of signal transduction

The particle can be in a free, reversibly bound state or irreversibly bound state, corresponding to the initialization of signal transduction. The first step in the algorithm for a free particle is to determine its state after a time-step Δt. This is done by using the probabilities given by $Q(\Delta t|x_0)$, $p(*,\Delta t|x_0)$ and $p(**,\Delta t|x_0)$. If the particle stays in a free state, the position of the particle is obtained by sampling its position according to $p(x,t|x_0)$ by the algorithm of Bignami and de Mattels, by setting

$$p_2(x,\Delta t \mid x_0) = \frac{\alpha(\gamma+\alpha)(\alpha+\beta)}{(\gamma-\alpha)(\alpha-\beta)} W\left(\frac{x+x_0}{\sqrt{4Dt}}, \alpha\sqrt{D\Delta t}\right) + \frac{\beta(\alpha+\beta)(\beta+\gamma)}{(\alpha-\beta)(\beta-\gamma)} W\left(\frac{x+x_0}{\sqrt{4Dt}}, \beta\sqrt{D\Delta t}\right) + \frac{\gamma(\beta+\gamma)(\gamma+\alpha)}{(\beta-\gamma)(\gamma-\alpha)} W\left(\frac{x+x_0}{\sqrt{4Dt}}, \gamma\sqrt{D\Delta t}\right) \quad (47)$$

The fact that $p_2(x,\Delta t|x_0)\leq 0$ is less obvious here. Since the reaction rate constants k_a, k_d and k_e are always positive (or zero), it would make no physical sense to have $p_2(x,\Delta t|x_0)>0$. Even though we were not able to prove formally that $p_2(x,\Delta t|x_0)\leq 0$, this assumption was verified for all our simulations.

If a particle is initially in a reversibly bound state, its state after the next timestep is determined by using the probabilities given by Q(Δt|*), p(*,Δt|*) and p(**,Δt|*). If the bound particle dissociates, the Green function p(x,Δt|*), which may also be written as the product of a Gaussian function by a function of three terms in Ω(x), is sampled by the rejection method.

$$p(x,\Delta t\,|\,*) = \frac{k_d}{D}\exp\left(-\frac{x^2}{4D\Delta t}\right)\left[\frac{\alpha}{(\gamma-\alpha)(\alpha-\beta)}\Omega\left(\frac{x}{\sqrt{4D\Delta t}}+\alpha\sqrt{D\Delta t}\right)\right. \qquad (48)$$
$$\left.+\frac{\beta}{(\alpha-\beta)(\beta-\gamma)}\Omega\left(\frac{x}{\sqrt{4D\Delta t}}+\beta\sqrt{D\Delta t}\right)+\frac{\gamma}{(\beta-\gamma)(\gamma-\alpha)}\Omega\left(\frac{x}{\sqrt{4D\Delta t}}+\gamma\sqrt{D\Delta t}\right)\right]$$

On Figure 4 (left), the probability distribution of a particle at x_0=2.5 from a membrane with k_a=5, k_d=1 and k_e=1 is shown for t=1,2,4,8 and 16. Simulation points obtained from sampling using the methods in this paper are also shown. The results are similar regardless the number of time-steps. On Figure 4 (right), the probabilities of a particle to be in a free, reversibly bound or irreversibly bound are shown for k_a=5, k_d=1 and k_e=0.01, 0.1 and 1. In all cases, since a particle will *always* reach the membrane at x=0 if given sufficient time, all particles will eventually bound irreversibly.

Figure 4

For transitions, the sampling algorithms are modified to use the special forms of the Green functions as discussed in Appendix A.

V. DISCUSSION AND CONCLUSION

We have discussed the interaction of a Brownian particle near a plane membrane with receptors, the most general case comprising the possibility of dissociation of the ligand-receptor complex and initiation of signal transduction. The simulation of particles histories using the BD algorithms described in this paper are able to reproduce accurately the theoretical distribution of distances from the membrane, the number of reversibly bound particles and the initiation of cell signaling following the analytical solution, regardless of the number of time-steps. The discretization of time for the simulation algorithm is an important benchmark for the calculation and for the self-consistency of theory. We were able to establish them, but were not able to verify all of them from their analytical forms. However, all of them were verified numerically. We have also developed algorithms which are very fast and require only a small amount of memory or disk space. These two very important aspects are usually not considered in related articles.

An important application of the theory described in this paper is the study of the response of a group of cells to ionizing radiation, specifically the role of TGFβ. TGFβ molecules are secreted by most cells in an inactive form called the LTGFβ and is rapidly converted to an active form by radiation or other stressors. TGFβ has been shown recently to suppress apoptosis in irradiated cell culture [11] and also to mediate cellular response to

DNA damage [34]. It could thus play an important role in the response of tissue to ionizing radiations [2]. The study of the role of TGFβ in cell culture is complicated by the fact that several isoforms of the molecule and of the receptor exist [33,35], and by its complex signaling pathways [36-37].

It is well known that ionizing radiation creates radical and molecular species ($^{\bullet}OH$, $H^{\bullet}$, H_2, H_2O_2, e^-_{aq},...) by the radiolysis of water in living matter in a highly non-homogeneous manner called the radiation track structure [38]. The $^{\bullet}OH$ radical liberates TGFβ molecules from its latent complex LTGFβ by triggering a conformational change [33]. Activated TGFβ binds to cells receptors and initiates signal transduction by the activation of a cascade of downstream signaling events mediated by Smad proteins. In this perspective, the simulations described in this paper are the first step in the implementation of a BD algorithm using reaction rate constants on cell surfaces to explain the experimental results on the role of TGFβ in irradiated cell cultures or tissues. These simulations will allow us to calculate range, lifetime and concentrations of activated TGFβ molecules as well as the number of affected cells and the positions where TGFβ molecules will bind to the cell surface receptors and initiate signal transduction following irradiation. This should provide considerable insight of the role of TGFβ in irradiated systems.

It is not possible at this time to compare our results with experimental data for several reasons, notably because they don't exist for the situations described in this paper. Nevertheless, this theoretical approach had a great success to explain chemical reaction kinetics [22-23] and in systems biology simulations [14-17]. We also have the necessary data (Table 1 and Table 2) to eventually use this approach with TGFβ in biological systems.

In future work, we plan to use radiation track structure models in different geometries of cell culture or tissue models to calculate the number of activated TGFβ and to include TGFβ signaling pathways in existing DNA repair models [39]. This will be possible by using the approach described in this paper with appropriate modifications for different geometries. These calculations will also be used to benchmark numerical calculations, making it possible to study more complex systems that are not amenable to analytic solutions. Differences between responses at high and low doses and random interactions of X-rays or electrons versus the distinct track structures of high-energy ions will be investigated. This should lead to significant improvement in our comprehension of radiation risk.

H. Acknowledgements

This work was supported by the NASA Space Radiation Risk Assessment project and the DoE Low Dose Program (DE-AI02-09ER64843). We also thank Drs. Noam Agmon, Walter Gautschi and Luc Devroye for useful correspondence.

References

[1] M. H. Barcellos-Hoff, Radiat. Res. Suppl. 150, S109 (1998).
[2] M. H. Barcellos-Hoff, C. Park and, E. G. Wright, Nat. Rev. Cancer **5**, 867 (2005).
[3] C. Mothersill and C. B. Seymour, Nat. Rev. Cancer **4**, 158–164 (2004).
[4] E. I. Azzam, S. M. De Toledo, D. R. Spitz, and J. B. Little, Cancer Res. **62**, 5436 (2002).
[5] H. Zhou, g. Randers-Pehrson, C. A. Waldren, D. Vannais, E. J. Hall et al, Proc. Nat. Acad. Sci. USA **97**, 2099 (2000).
[6] C. Mothersill and C. B. Seymour, Int J Radiat Biol **71**, 421 (1997).
[7] F. M. Lyng, C. B. Seymour, and C. Mothersill, Br J Cancer **83**, 1223 (2000).
[8] J. L. Redpath, S. C. Short, M. Woodcock, and P. J. Johnson, Radiat. Res. 159, 433 (2003).
[9] F. A. Cucinotta and L. J. Chappell, Mut. Res. **687**, 49 (2010).
[10] M. B. Sporn and G. J. Torado, N Eng J Med **303**, 878 (1980).
[11] D. I. Portess, G. Bauer, M. A. Hill, and P. O'Neill, Cancer Res. **67**, 1246 (2007).
[12] H. Matsumoto, S. Hayashi, M. Hatashita, K. Ohnishi, H. Shioura, T. Ohtsubo, R. Kitai, T. Ohnishi, and E. Kano, Radiat. Res. **155**, 387 (2001).
[13] J. B. Little, E. I. Azzam, S. M. de Toledo, and H. Nagasawa, Radiat. Prot. Dosim. **99**, 159 (2002).
[14] L. Batsilas, A. M. Berezhkovskii, and Y. Shvartsman, Biophys. J. **85**, 1(2003).
[15] S. H. Wiley, S. Y. Shvartsman, and D. A. Lauffenburger, TRENDS in Cell Biology **13**, 43 (2003).
[16] M. I. Monine, A. M. Berezhkovskii, E. J. Joslin, S. H. Wiley, D. A. Lauffenburger, and S. Y. Shvartsman, Biophys. J. **88**, 2384 (2005).
[17] S. Y. Shvartsman, S. H. Wiley, W. H. Deen, and D. A. Lauffenburger, Biophys. J. 81, 1851 (2001).
[18] G. Lamm and K. Schulten, J. Chem. Phys. **78**, 2713 (1983).
[19] N. Agmon, J. Chem. Phys. **81**, 2811 (1984).
[20] N. Agmon, E. Pines, and D. Huppert, J. Chem. Phys. **88**, 5631 (1988).
[21] A. L. Edelstein and N. Agmon, J. Chem. Phys. **99**, 5396 (1993).
[22] H. Kim, K. J. Shin, and N. Agmon, J. Chem. Phys. **111**, 3791 (1999).
[23] S. Park and N. Agmon, J. Phys. Chem. B **112**, 5977 (2008).
[24] D. C. Clarke DC and X. Lui, TRENDS in Cell. Biol. **18**, 430 (2008).
[25] A. M. Berezhkovskii, Y. A. Makhnovskii, M. I. Monine, V. Y. Zitserman, and S. Y. Shvartsman, J. Chem. Phys. **22**, 11390 (2004).
[26] G. P. Poppe and C. M. J. Wijers, ACM Trans. Math Software 16, 47 (1990).
[27] I. Plante, Radiat. Env. Biophys. **50**, 389 (2011).
[28] See Supplemental Material at [URL will be inserted by the publisher] for verification of time discretization equations using Mathematica.
[29] See Supplemental Material at [URL will be inserted by the publisher] for proofs of the time discretization equations.
[30] I. S. Gradsteyn and I. M. Ryzhik, *Table of Integrals, Series and Product*. 7th edition. (Academic Press, New York, 2007)
[31] L. Devroye, *Non-Uniform Variate Generation* (Springer-Verlag, New York, 1986).
[32] A. Bignami and A. de Mattels A, J. Inst. Math. Appl. **8**, 80 (1971).

[33] M. F. Jobling, J. D. Mott, M. T. Finnegan, V. Jurukovski et al., Radiat. Res. **166**, 839 (2006).
[34] M. Durante and F. A. Cucinotta, Nat. Rev. Cancer **8**, 1 (2008).
[35] J. M. G. Vilar, R. Jansen and C. Sander, PLoS Comput. Biol. **2**, 36 (2006).
[36] S. S. Prime, M. Pring, M. Davies, and I. C. Paterson, Crit. Rev. Oral Biol. Med. **15**, 324 (2004).
[37] P. Melke, H. Jönsson, E. Pardali, P. ten Dijke, and C. Peterson, Biophys. J. **91**, 4368 (2006).
[38] Y. Muroya, I. Plante, E. I. Azzam, J. Meesungnoen, Y. Katsumura, and J.-P. Jay-Gerin, Radiat. Res. **165**, 485 (2006).
[39] F. A. Cucinotta, J. M. Pluth, J. A. Anderson, J. V. Harper, P. O'Neill, Radiat. Res. **169**, 214 (2008).
[40] K. B. Ewan, R. L. Henshall-Powell, S. A. Ravani, M. Jose Pajares, et al., Cancer Res. **62**, 5627 (2002).

Figure captions

Figure 1: Probability distribution of a particle near a reflecting boundary for x_0=2.5 and D=1 at t=1, 2, 4, 8 and 16 units. The lines are the analytical predictions $p_{ref}(x,t|x_0)$. The dots are given by the simulation of 10^6 particles histories either with one or multiple time-steps.

Figure 2: (Left) Probability distribution of a particle near a partially absorbing and reflecting boundary for x_0=2.5, k_a=5 and D=1 at t=1, 2, 4, 8 and 16 units. The lines are the analytical predictions $p(x,t|x_0)$. The dots are given by the simulation of 10^6 particles histories either with one or multiple time-steps. (Right) Probability of a particle initially at x_0=2.5 to be free or irreversibly bound as a function of time for k_a=5.

Figure 3: (Left) Probability distribution of a particle near a partially absorbing and reflecting boundary with back reaction for x_0=2.5, k_a=5, k_d=1 and D=1 at t=1, 2, 4, 8 and 16 s. The coefficients $\alpha\approx4.7913$ and $\beta\approx0.20872$. The lines are the analytical predictions $p(x,t|x_0)$. The dots are given by the simulation of 10^6 particles histories either with one or multiple time-steps. (Right) Probability of a particle initially at x_0=2.5 to be free or reversibly bound as a function of time for k_a=5 and k_d=0.1, 1 and 10.

Figure 4: (Left) Probability distribution of a particle near a partially absorbing and reflecting boundary with back reaction for x_0=2.5, k_a=5, k_d=1 and D=1 at t=1, 2, 4, 8 and 16 s. The coefficients $\alpha\approx4.8$, $\beta\approx0.099827+1.01569i$ and $\gamma\approx0.099827-1.01569i$. The lines are the analytical predictions $p(x,t|x_0)$. The dots are given by the simulation of 10^6 particles histories either with one or multiple time-steps. (Right) Probability of a particle initially at x_0=2.5 to be free, reversibly bound or irreversibly bound as a function of time for k_a=5, k_d=1 and k_e=0.1, 1 and 10.

Figure 1

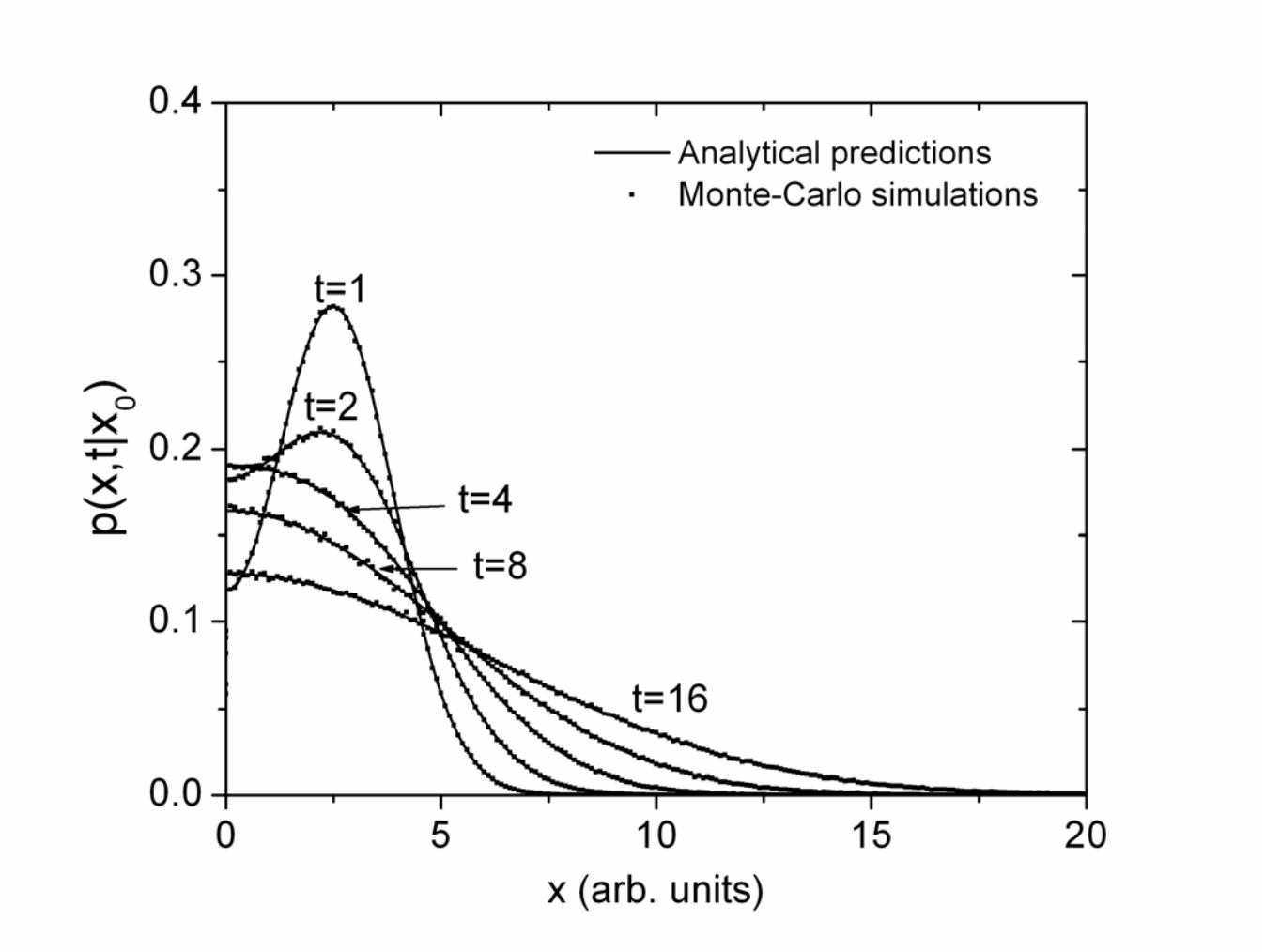
Analytical predictions
Monte-Carlo simulations
t=1
t=2
t=4
t=8
t=16
p(x,t|x0)
x (arb. units)
0.0
0.1
0.2
0.3
0.4
0
5
10
15
20

Figure 2

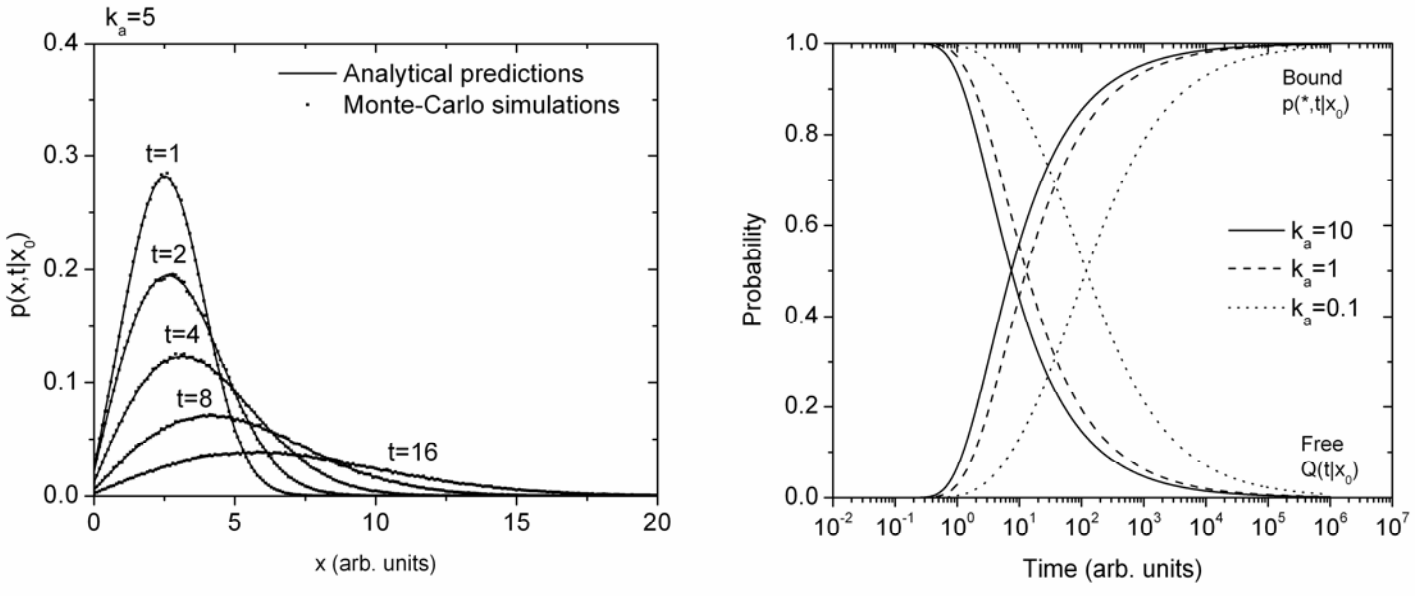
k_a=5
Analytical predictions
Monte-Carlo simulations
t=1
t=2
t=4
t=8
t=16
p(x,t|x_0)
x (arb. units)
Bound
p(*,t|x_0)
k_a=10
k_a=1
k_a=0.1
Free
Q(t|x_0)
Probability
Time (arb. units)

Figure 3

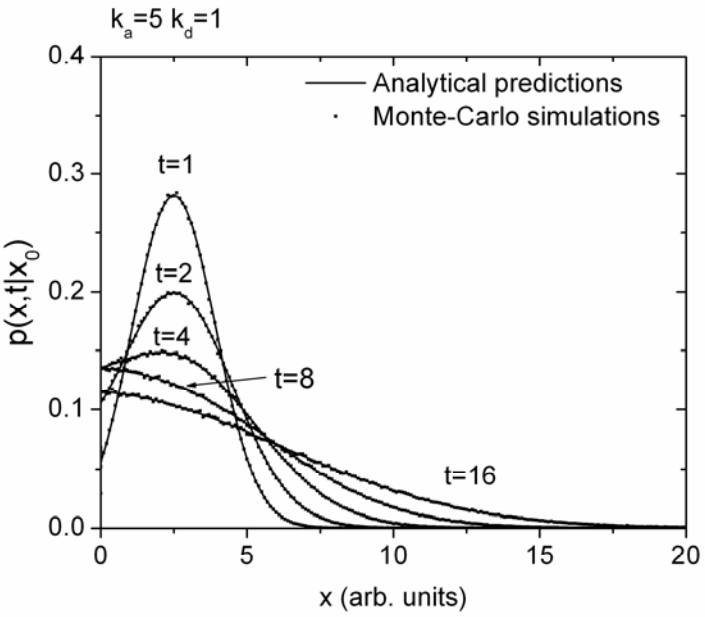
k_a=5 k_d=1
Analytical predictions
Monte-Carlo simulations
t=1
t=2
t=4
t=8
t=16
p(x,t|x_0)
x (arb. units)

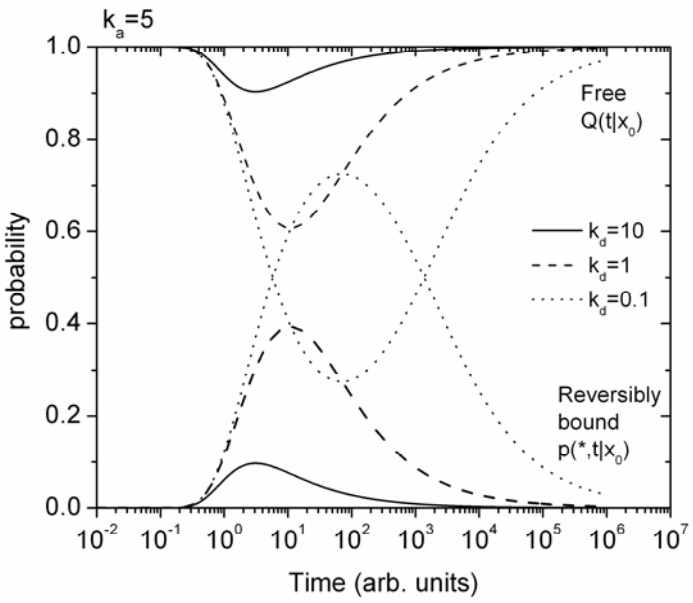
k_a=5
Free
Q(t|x_0)
k_d=10
k_d=1
k_d=0.1
Reversibly
bound
p(*,t|x_0)
probability
Time (arb. units)

Figure 4

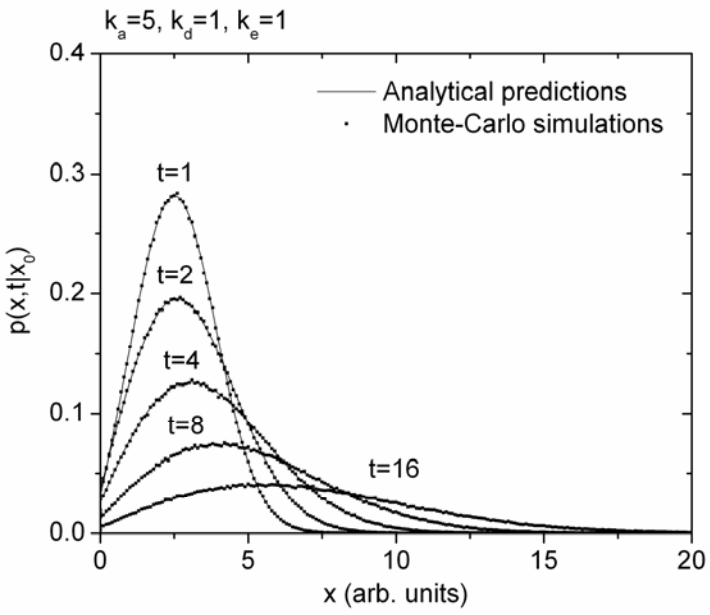
k_a=5, k_d=1, k_e=1
Analytical predictions
Monte-Carlo simulations
t=1
t=2
t=4
t=8
t=16
p(x,t|x_0)
x (arb. units)

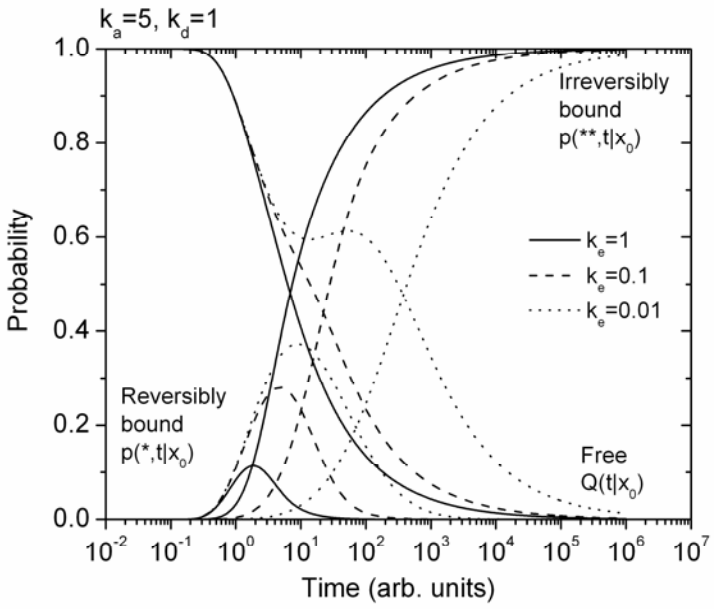
k_a=5, k_d=1
Irreversibly bound p(**,t|x_0)
k_e=1
k_e=0.1
k_e=0.01
Reversibly bound p(*,t|x_0)
Free Q(t|x_0)
Probability
Time (arb. units)

Table 1. Parameters used for TGFβ

Parameter	Description	Value	Reference
D	Ligand diffusivity	2.6×10^{-7} cm^2/s	
A	Culture surface	10 cm^2	[15]
h	Height of the extracellular medium	0.2 cm	[15]
k_e	Complex internalization rate constant	3 min^{-1} = 0.05 s^{-1}	[40]
k_{on}	Forward binding rate constant	$(2.3 \pm 0.2) \times 10^7$ M^{-1}s^{-1}	[24]
k_d	Complex dissociation rate constant	$(1.5 \pm 0.2) \times 10^{-4}$ s^{-1}	[24]
R_0	Number of receptors at cell surface	1000	[24]
R_{cell}	Radius of the cell	0.0025 cm	[15]
N_{cells}	Number of cells in culture	100000	[15]

Table 2. Calculated quantities

Parameter	Description	Value	Reference
σ	Fraction of culture surface covered by cells	0.196	[16]
k_a	Rate constant at the cell surface	8.46×10^{-4} cm s^{-1}	
κ_{cell}	Surface trapping rate	3.18×10^{-4} cm s^{-1}	

Appendix A: Transitions

The Green functions described in sections 2.4 and 2.5 may have singularities (0/0) when values of α, β and/or γ are equal. The Green functions takes different forms for these values.

I.1 Reversible binding with membrane at x=0

Equations (13) and (14) are still adequate for complex values of α and β, since the imaginary terms cancels to 0, but there is a singularity when α=β (or Δ=0). By taking the limit β→α of equations (13) we find[5]:

$$\lim_{\beta\to\alpha} p(x,t\mid x_0) = p_{ref}(x,t\mid x_0) - 2\alpha^2 W'\left(\frac{x+x_0}{\sqrt{4Dt}}, \alpha\sqrt{Dt}\right) - 2\alpha W\left(\frac{x+x_0}{\sqrt{4Dt}}, \alpha\sqrt{Dt}\right) \tag{A1}$$

The probability of survival, in this case, can be obtained either by taking the limit β→α of equation (14) or by integrating equation (A1). This yields:

$$\lim_{\beta\to\alpha} Q(t\mid x_0) = 1 + 2\alpha W'\left(\frac{x_0}{\sqrt{4Dt}}, \alpha\sqrt{Dt}\right) \tag{A2}$$

We may proceed as in section II or take the limit β→α of equations (15), (16), (17) and (18). Either approach yields:

$$\lim_{\beta\to\alpha} p(*,t\mid x_0) = -2\alpha W'\left(\frac{x_0}{\sqrt{4Dt}}, \alpha\sqrt{Dt}\right) \tag{A3}$$

$$\lim_{\beta\to\alpha} p(x,t\mid *) = -\alpha^2 W'\left(\frac{x}{\sqrt{4Dt}}, \alpha\sqrt{Dt}\right) \tag{A4}$$

The Green function for dissociation can also be written in a convenient form for rejection sampling by using the Gaussian function as a common factor:

$$\lim_{\beta\to\alpha} p(x,t\mid *) = 2\alpha^2\sqrt{\frac{Dt}{\pi}}e^{-\frac{x^2}{4Dt}}\left[1-(2\alpha Dt+x)\sqrt{\frac{\pi}{4Dt}}\Omega\left(\frac{x}{\sqrt{4Dt}}+\alpha\sqrt{Dt}\right)\right] \tag{A4'}$$

$$\lim_{\beta\to\alpha} Q(t\mid *) = 1 + \alpha\Omega'\left(\alpha\sqrt{Dt}\right) - \Omega\left(\alpha\sqrt{Dt}\right) \tag{A5}$$

$$\lim_{\beta\to\alpha} p(*,t\mid *) = -\alpha\Omega'\left(\alpha\sqrt{Dt}\right) + \Omega\left(\alpha\sqrt{Dt}\right) \tag{A6}$$

where Ω'(x)=W'(0,x).

[5] The following equations are greatly simplified by introducing the function

$$W'\left(\frac{x+x_0}{\sqrt{4Dt}}, \alpha\sqrt{Dt}\right) \equiv -2\sqrt{\frac{Dt}{\pi}}e^{-\frac{(x-x_0)^2}{4Dt}} + (2\alpha Dt + x + x_0)W\left(\frac{x+x_0}{\sqrt{4Dt}}, \alpha\sqrt{Dt}\right)$$

I.2 Reversible recombination with membrane and activation of signal transduction

Since α, β and γ are the roots of a 3rd degree polynomial, there are much more transitions to consider. A "first order" transition occurs when one root vanishes (equals 0); a "second order" transition occurs when two roots are equal; a "third order" transition occurs when all three roots have the same identical real part. These cases are discussed in this section.

I.2.1 First order transition

In this case, one of the roots is zero (suppose γ=0). The two other roots are different and are not equal to zero, since this would be a 2nd or 3rd order transition. From equation (27c), either k_a or k_e is 0. Setting k_a=0 would have no physical sense since a free particle cannot bind to the membrane. Hence we need to set k_e=0, which is the situation described in section 2.4. Using γ=0 in the Green functions of section 2.5 gives the Green functions of section 2.4.

I.2.2 Second order transition

This occurs when two roots, say α and β, are equal. This implies that all roots must be real. In this case, the first two terms of equation (23) may be written as 0/0. This ambiguity is solved by calculating the limit of $p(x,t|x_0)$ with $\beta\to\alpha$. We find:

$$\lim_{\beta\to\alpha} p(x,t\mid x_0) = p_{ref}(x,t\mid x_0) - 2\alpha^2\frac{\alpha+\gamma}{\alpha-\gamma}W'\left(\frac{x+x_0}{\sqrt{4Dt}},\alpha\sqrt{Dt}\right) - 2\alpha\frac{\alpha^2-2\alpha\gamma-\gamma^2}{(\alpha-\gamma)^2}W\left(\frac{x+x_0}{\sqrt{4Dt}},\alpha\sqrt{Dt}\right) \quad \text{(A7)}$$
$$-\frac{\gamma(\alpha+\gamma)^2}{(\alpha-\gamma)^2}W\left(\frac{x+x_0}{\sqrt{4Dt}},\gamma\sqrt{Dt}\right)$$

The probability of survival $Q(t|x_0)$ can be calculated either by integrating (A7) or by the limit of equation (24) with $\beta\to\alpha$. We find:

$$\lim_{\beta\to\alpha} Q(t\mid x_0) = 1 - W\left(\frac{x_0}{\sqrt{4Dt}},0\right) + \frac{2\alpha(\alpha+\gamma)}{(\alpha-\gamma)}W'\left(\frac{x_0}{\sqrt{4Dt}},\alpha\sqrt{Dt}\right) - \frac{4\alpha\gamma}{(\alpha-\gamma)^2}W\left(\frac{x_0}{\sqrt{4Dt}},\alpha\sqrt{Dt}\right) \quad \text{(A8)}$$
$$+\left(\frac{\gamma+\alpha}{\gamma-\alpha}\right)^2 W\left(\frac{x_0}{\sqrt{4Dt}},\gamma\sqrt{Dt}\right)$$

Similarly, the other Green functions are:

$$\lim_{\beta\to\alpha} p(*,t\mid x_0) = -\frac{\alpha(2\alpha+\gamma)}{\alpha-\gamma}W'\left(\frac{x_0}{\sqrt{4Dt}},\alpha\sqrt{Dt}\right) + \frac{\gamma(2\alpha+\gamma)}{(\alpha-\gamma)^2}W\left(\frac{x_0}{\sqrt{4Dt}},\alpha\sqrt{Dt}\right) - \frac{\gamma(2\alpha+\gamma)}{(\alpha-\gamma)^2}W\left(\frac{x_0}{\sqrt{4Dt}},\gamma\sqrt{Dt}\right) \quad \text{(A9)}$$

$$\lim_{\beta\to\alpha} p(**,t\mid x_0) = -\frac{\alpha\gamma}{\alpha-\gamma}W'\left(\frac{x_0}{\sqrt{4Dt}},\alpha\sqrt{Dt}\right) + \frac{(2\alpha-\gamma)\gamma}{(\alpha-\gamma)^2}W\left(\frac{x_0}{\sqrt{4Dt}},\alpha\sqrt{Dt}\right) - \frac{\alpha^2}{(\alpha-\gamma)^2}W\left(\frac{x_0}{\sqrt{4Dt}},\gamma\sqrt{Dt}\right) \quad \text{(A10)}$$
$$+W\left(\frac{x_0}{\sqrt{4Dt}},0\right)$$

By summing individually each term of (A8-A10) we can verify that $Q(t|x_0)+p(*,t|x_0)+p(**,t|x_0)=1$.

$$\lim_{\beta\to\alpha} p(x,t\,|\,*) = \frac{2\alpha(\alpha+\gamma)^2}{(2\alpha+\gamma)(\alpha-\gamma)^2}\left[\alpha(\gamma-\alpha)W'\left(\frac{x}{\sqrt{4Dt}},\alpha\sqrt{Dt}\right)+\gamma W\left(\frac{x}{\sqrt{4Dt}},\alpha\sqrt{Dt}\right)-\gamma W\left(\frac{x}{\sqrt{4Dt}},\gamma\sqrt{Dt}\right)\right] \quad (A11)$$

The last equation can be also be rewritten in a form convenient for rejection sampling by putting a Gaussian factor in evidence. For the reversibly bound particle, we have:

$$\lim_{\beta\to\alpha} Q(t\,|\,*) = \frac{2\alpha(\alpha+\gamma)^2}{2\alpha+\gamma}\left[\frac{1}{\alpha-\gamma}\Omega'\left(\alpha\sqrt{Dt}\right)-\frac{1}{(\alpha-\gamma)^2}\Omega\left(\alpha\sqrt{Dt}\right)+\frac{1}{(\alpha-\gamma)^2}\Omega\left(\gamma\sqrt{Dt}\right)\right] \quad (A12)$$

$$\lim_{\beta\to\alpha} p(*,t\,|\,*) = -\frac{\alpha(\alpha+\gamma)}{(\alpha-\gamma)}\Omega'\left(\alpha\sqrt{Dt}\right)+\frac{\alpha^2+\gamma^2}{(\alpha-\gamma)^2}\Omega\left(\alpha\sqrt{Dt}\right)-\frac{2\alpha\gamma}{(\alpha-\gamma)^2}\Omega\left(\gamma\sqrt{Dt}\right) \quad (A13)$$

$$\lim_{\beta\to\alpha} p(**,t\,|\,*) = 1+\frac{\alpha\gamma(\alpha+\gamma)}{(2\alpha+\gamma)(\alpha-\gamma)}\Omega'\left(\alpha\sqrt{Dt}\right)+\frac{\gamma(3\alpha^2-\gamma^2)}{(2\alpha+\gamma)(\alpha-\gamma)^2}\Omega\left(\alpha\sqrt{Dt}\right)-\frac{2\alpha^3}{(2\alpha+\gamma)(\alpha-\gamma)^2}\Omega\left(\gamma\sqrt{Dt}\right) \quad (A14)$$

By summing each term individually, as expected, Q(t|*)+p(*,t|*)+p(**,t|*)=1. Two cases are possible. The first case is $\alpha=\beta=0$ and $\gamma\neq0$. Equation (22) implies that $\gamma=k_a/D$ and $k_e=k_d=0$. This is the partially absorptive boundary at x=0, which has already been discussed in section 2.3. The second possible case is $\alpha=\beta\neq0$ and $\gamma=0$. This is the transition of the reversible boundary, discussed in Appendix I.1. If $\gamma=0$, the last expressions can be simplified to yield the equations described in the first part of this appendix.

I.2.3 Third order transition

A 3rd order transition imposes severe conditions on the rate constants, since the real part of the roots are equal. The trivial case $k_a=k_d=k_e=0$ is the reflective boundary. Otherwise, the roots can be expressed as $\alpha=r_p$, $\beta=r_p+\sqrt{-1}\,i_p$ and $\gamma=r_p-\sqrt{-1}\,i_p$. From equation (22a), since k_a is real and positive, the real part of the roots are given by $r_p=k_a/3D$. The rate constant k_e cannot be 0, since one of the roots would have to be identically equal to 0 this would not be a 3rd order transition. Equation (22c) allows the calculation of the imaginary part i_p,

$$i_p = \frac{1}{3D}\sqrt{27Dk_e-k_a^2} \quad (A16)$$

For a 3rd order transition, equation (22b) imposes the following condition on k_d :

$$k_e = \frac{-2k_a^2+9Dk_d}{18D} \quad (A17)$$

A 3rd order transition with real coefficients could be met by setting, for example, $k_a=9$, $k_d=24$, $k_e=3$ and $D=1$, which would give $\alpha=\beta=\gamma=3$. Strict conditions like this are not expected to happen in real life; thus, this is more a theoretical curiosity.

For calculations, if two roots are complex conjugate with imaginary part different from 0, there are no division by 0 in any of the Green functions; the general equations can thus be used without any modification. However, if all roots are equal and real, the limit $\beta\to\alpha$ and $\gamma\to\alpha$ should be used to avoid a division by 0. After a long calculation, we find[6]:

$$\lim_{\substack{\beta\to\alpha\\ \gamma\to\alpha}} p(x,t\mid x_0) = p_{ref}(x,t\mid x_0) - 2\alpha^3 W''\left(\frac{x+x_0}{\sqrt{4Dt}},\alpha\sqrt{Dt}\right) - 6\alpha^2 W'\left(\frac{x+x_0}{\sqrt{4Dt}},\alpha\sqrt{Dt}\right) - 3\alpha W\left(\frac{x+x_0}{\sqrt{4Dt}},\alpha\sqrt{Dt}\right) \quad \text{(A18)}$$

$$\lim_{\substack{\beta\to\alpha\\ \gamma\to\alpha}} Q(t\mid x_0) = 1 - W\left(\frac{x_0}{\sqrt{4Dt}},0\right) + 2\alpha^2 W''\left(\frac{x_0}{\sqrt{4Dt}},\alpha\sqrt{Dt}\right) + 2\alpha W'\left(\frac{x_0}{\sqrt{4Dt}},\alpha\sqrt{Dt}\right) + W\left(\frac{x_0}{\sqrt{4Dt}},\alpha\sqrt{Dt}\right) \quad \text{(A19)}$$

$$\lim_{\substack{\beta\to\alpha\\ \gamma\to\alpha}} p(*,t\mid x_0) = -\frac{3\alpha^2}{2} W''\left(\frac{x_0}{\sqrt{4Dt}},\alpha\sqrt{Dt}\right) - 3\alpha W'\left(\frac{x_0}{\sqrt{4Dt}},\alpha\sqrt{Dt}\right) \quad \text{(A20)}$$

$$\lim_{\substack{\beta\to\alpha\\ \gamma\to\alpha}} p(**,t\mid x_0) = W\left(\frac{x_0}{\sqrt{4Dt}},0\right) - \frac{\alpha^2}{2} W''\left(\frac{x_0}{\sqrt{4Dt}},\alpha\sqrt{Dt}\right) + \alpha W'\left(\frac{x_0}{\sqrt{4Dt}},\alpha\sqrt{Dt}\right) - W\left(\frac{x_0}{\sqrt{4Dt}},\alpha\sqrt{Dt}\right) \quad \text{(A21)}$$

The condition $Q(t|x_0)+p(*,t|x_0)+p(**,t|x_0)=1$ is also verified by equations (A19-A21). For the bound particle, the Green function for dissociation is:

$$\lim_{\substack{\beta\to\alpha\\ \gamma\to\alpha}} p(x,t\mid *) = -\frac{4\alpha^3}{2} W''\left(\frac{x}{\sqrt{4Dt}},\alpha\sqrt{Dt}\right) - \frac{8\alpha^2}{3} W'\left(\frac{x}{\sqrt{4Dt}},\alpha\sqrt{Dt}\right) \quad \text{(A22)}$$

As a common Gaussian factor can also be put in evidence for both functions W' and W" to sample equation (A22) by rejection. The probabilities for the bound particle can also be calculated for a 3rd order transition:

$$\lim_{\substack{\beta\to\alpha\\ \gamma\to\alpha}} Q(t\mid *) = \frac{4}{3}\alpha^2 \Omega''\left(\alpha\sqrt{Dt}\right) \quad \text{(A23)}$$

$$\lim_{\substack{\beta\to\alpha\\ \gamma\to\alpha}} p(*,t\mid *) = \Omega\left(\alpha\sqrt{Dt}\right) - \alpha\Omega'\left(\alpha\sqrt{Dt}\right) - \alpha^2\Omega''\left(\alpha\sqrt{Dt}\right) \quad \text{(A24)}$$

$$\lim_{\substack{\beta\to\alpha\\ \gamma\to\alpha}} p(**,t\mid *) = 1 - \Omega\left(\alpha\sqrt{Dt}\right) + \alpha\Omega'\left(\alpha\sqrt{Dt}\right) - \frac{\alpha^2}{3}\Omega''\left(\alpha\sqrt{Dt}\right) \quad \text{(A25)}$$

where $\Omega''(x)=W''(0,x)$. Once again, $Q(t|*)+p(*,t|*)+p(**,t|*)=1$.

---

[6] The equations of the 3rd order transition are greatly simplified by introducing the functions

$$W''\left(\frac{x+x_0}{\sqrt{4Dt}},\alpha\sqrt{Dt}\right) \equiv -2(2\alpha Dt + x + x_0)\sqrt{\frac{Dt}{\pi}} e^{-\frac{(x-x_0)^2}{4Dt}} + \left\{4\alpha^2(Dt)^2 + (x+x_0)^2 + 2Dt\left[1+2\alpha(x+x_0)\right]\right\} W\left(\frac{x+x_0}{\sqrt{4Dt}},\alpha\sqrt{Dt}\right)$$

Appendix B: Algorithm of Bignami and de Mattels

The negative mixture algorithm of Bignami and de Mattels (1971) is described here. If a given probability density f(x) can be written as follows

$$f(x) = \sum_i p_i f_i(x)$$

where the $f_i(x)$'s are probability densities, but the p_i's are real numbers summing to 1. The p_i's can be decomposed into positive and negative parts, p_{i+} and p_{i-}. In this case,

$$f(x) \le g(x) = \sum_i p_{i+} f_i(x)$$

The following rejection algorithm can be used:

BEGIN
REPEAT

Generate a random variate X with density $\sum_i p_{i+} f_i(x) / \sum_i p_{i+}$

Generate a uniform [0,1] random variate U

UNTIL $U \sum_i p_{i+} f_i(X) \le \sum_i p_i f_i(X)$
RETURN X ■